Observation of a near-threshold $\omega J/\psi$ mass enhancement in exclusive $B \to K\omega J/\psi$ decays

K. Abe, ¹⁰ K. Abe, ⁴⁶ N. Abe, ⁴⁹ I. Adachi, ¹⁰ H. Aihara, ⁴⁸ M. Akatsu, ²⁴ Y. Asano, ⁵³ T. Aso,⁵² V. Aulchenko,² T. Aushev,¹⁴ T. Aziz,⁴⁴ S. Bahinipati,⁶ A. M. Bakich,⁴³ Y. Ban,³⁶ M. Barbero,⁹ A. Bay,²⁰ I. Bedny,² U. Bitenc,¹⁵ I. Bizjak,¹⁵ S. Blyth,²⁹ A. Bondar, A. Bozek, M. Bračko, 22, 15 J. Brodzicka, T. E. Browder, M.-C. Chang, 29 P. Chang,²⁹ Y. Chao,²⁹ A. Chen,²⁶ K.-F. Chen,²⁹ W. T. Chen,²⁶ B. G. Cheon,⁴ R. Chistov, ¹⁴ S.-K. Choi, ⁸ Y. Choi, ⁴² Y. K. Choi, ⁴² A. Chuvikov, ³⁷ S. Cole, ⁴³ M. Danilov, ¹⁴ M. Dash, ⁵⁵ L. Y. Dong, ¹² R. Dowd, ²³ J. Dragic, ²³ A. Drutskoy, ⁶ S. Eidelman, Y. Enari, 4 D. Epifanov, C. W. Everton, 5 F. Fang, S. Fratina, 15 H. Fujii, ¹⁰ N. Gabyshev, ² A. Garmash, ³⁷ T. Gershon, ¹⁰ A. Go, ²⁶ G. Gokhroo, ⁴⁴ B. Golob, ^{21,15} M. Grosse Perdekamp, ³⁸ H. Guler, ⁹ J. Haba, ¹⁰ F. Handa, ⁴⁷ K. Hara, ¹⁰ T. Hara, ³⁴ N. C. Hastings, ¹⁰ K. Hasuko, ³⁸ K. Hayasaka, ²⁴ H. Hayashii, ²⁵ M. Hazumi, ¹⁰ E. M. Heenan, ²³ I. Higuchi, ⁴⁷ T. Higuchi, ¹⁰ L. Hinz, ²⁰ T. Hojo, ³⁴ T. Hokuue, ²⁴ Y. Hoshi, 46 K. Hoshina, 51 S. Hou, 26 W.-S. Hou, 29 Y. B. Hsiung, 29 H.-C. Huang, 29 T. Igaki, ²⁴ Y. Igarashi, ¹⁰ T. Iijima, ²⁴ A. Imoto, ²⁵ K. Inami, ²⁴ A. Ishikawa, ¹⁰ H. Ishino, ⁴⁹ K. Itoh, ⁴⁸ R. Itoh, ¹⁰ M. Iwamoto, ³ M. Iwasaki, ⁴⁸ Y. Iwasaki, ¹⁰ R. Kagan, ¹⁴ H. Kakuno, ⁴⁸ J. H. Kang,⁵⁶ J. S. Kang,¹⁷ P. Kapusta,³⁰ S. U. Kataoka,²⁵ N. Katayama,¹⁰ H. Kawai,³ H. Kawai, ⁴⁸ Y. Kawakami, ²⁴ N. Kawamura, ¹ T. Kawasaki, ³² N. Kent, ⁹ H. R. Khan, ⁴⁹ A. Kibayashi,⁴⁹ H. Kichimi,¹⁰ H. J. Kim,¹⁹ H. O. Kim,⁴² Hyunwoo Kim,¹⁷ J. H. Kim,⁴² S. K. Kim, ⁴¹ T. H. Kim, ⁵⁶ K. Kinoshita, ⁶ P. Koppenburg, ¹⁰ S. Korpar, ^{22,15} P. Križan, ^{21,15} P. Krokovny,² R. Kulasiri,⁶ C. C. Kuo,²⁶ H. Kurashiro,⁴⁹ E. Kurihara,³ A. Kusaka,⁴⁸ A. Kuzmin,² Y.-J. Kwon,⁵⁶ J. S. Lange,⁷ G. Leder,¹³ S. E. Lee,⁴¹ S. H. Lee,⁴¹ Y.-J. Lee, 29 T. Lesiak, 30 J. Li, 40 A. Limosani, 23 S.-W. Lin, 29 D. Liventsev, 14 J. MacNaughton, ¹³ G. Majumder, ⁴⁴ F. Mandl, ¹³ D. Marlow, ³⁷ T. Matsuishi, ²⁴ H. Matsumoto, ³² S. Matsumoto, ⁵ T. Matsumoto, ⁵⁰ A. Matyja, ³⁰ Y. Mikami, ⁴⁷ W. Mitaroff, ¹³ K. Miyabayashi, ²⁵ Y. Miyabayashi, ²⁴ H. Miyake, ³⁴ H. Miyata, ³² R. Mizuk, ¹⁴ D. Mohapatra, ⁵⁵ G. R. Moloney, ²³ G. F. Moorhead, ²³ T. Mori, ⁴⁹ A. Murakami, ³⁹ T. Nagamine, ⁴⁷ Y. Nagasaka, ¹¹ T. Nakadaira, ⁴⁸ I. Nakamura, ¹⁰ E. Nakano, ³³ M. Nakao, ¹⁰ H. Nakazawa, ¹⁰ Z. Natkaniec, ³⁰ K. Neichi, ⁴⁶ S. Nishida, ¹⁰ O. Nitoh, ⁵¹ S. Noguchi, ²⁵ T. Nozaki, ¹⁰ A. Ogawa, ³⁸ S. Ogawa, ⁴⁵ T. Ohshima, ²⁴ T. Okabe, ²⁴ S. Okuno, ¹⁶ S. L. Olsen, Y. Onuki, W. Ostrowicz, H. Ozaki, P. Pakhlov, H. Palka, Ozaki, D. Pakhlov, H. Palka, D. Pakhlov, M. Palka, D. Pakhlov, H. Palka, D. Pakhlov, M. Palka, D. Pakhlov, D. Pakhlov, D. Pakhlov, M. Palka, D. Pakhlov, C. W. Park, 42 H. Park, 19 K. S. Park, 42 N. Parslow, 43 L. S. Peak, 43 M. Pernicka, 13 J.-P. Perroud,²⁰ M. Peters,⁹ L. E. Piilonen,⁵⁵ A. Poluektov,² F. J. Ronga,¹⁰ N. Root,² M. Rozanska, 30 H. Sagawa, 10 M. Saigo, 47 S. Saitoh, 10 Y. Sakai, 10 H. Sakamoto, 18 T. R. Sarangi, ¹⁰ M. Satapathy, ⁵⁴ N. Sato, ²⁴ O. Schneider, ²⁰ J. Schümann, ²⁹ C. Schwanda, ¹³ A. J. Schwartz, T. Seki, S. Semenov, K. Senyo, Y. Settai, R. Seuster, M. E. Sevior, ²³ T. Shibata, ³² H. Shibuya, ⁴⁵ B. Shwartz, ² V. Sidorov, ² V. Siegle, ³⁸ J. B. Singh, ³⁵ A. Somov, ⁶ N. Soni, ³⁵ R. Stamen, ¹⁰ S. Stanič, ^{53,*} M. Starič, ¹⁵ A. Sugi, ²⁴ A. Sugiyama,³⁹ K. Sumisawa,³⁴ T. Sumiyoshi,⁵⁰ S. Suzuki,³⁹ S. Y. Suzuki,¹⁰ O. Tajima,¹⁰ F. Takasaki, ¹⁰ K. Tamai, ¹⁰ N. Tamura, ³² K. Tanabe, ⁴⁸ M. Tanaka, ¹⁰ G. N. Taylor, ²³

Y. Teramoto,³³ X. C. Tian,³⁶ S. Tokuda,²⁴ S. N. Tovey,²³ K. Trabelsi,⁹ T. Tsuboyama,¹⁰ T. Tsukamoto,¹⁰ K. Uchida,⁹ S. Uehara,¹⁰ T. Uglov,¹⁴ K. Ueno,²⁹ Y. Unno,³ S. Uno,¹⁰ Y. Ushiroda,¹⁰ G. Varner,⁹ K. E. Varvell,⁴³ S. Villa,²⁰ C. C. Wang,²⁹ C. H. Wang,²⁸ J. G. Wang,⁵⁵ M.-Z. Wang,²⁹ M. Watanabe,³² Y. Watanabe,⁴⁹ L. Widhalm,¹³ Q. L. Xie,¹² B. D. Yabsley,⁵⁵ A. Yamaguchi,⁴⁷ H. Yamamoto,⁴⁷ S. Yamamoto,⁵⁰ T. Yamanaka,³⁴ Y. Yamashita,³¹ M. Yamauchi,¹⁰ Heyoung Yang,⁴¹ P. Yeh,²⁹ J. Ying,³⁶ K. Yoshida,²⁴ Y. Yuan,¹² Y. Yusa,⁴⁷ H. Yuta,¹ S. L. Zang,¹² C. C. Zhang,¹² J. Zhang,¹⁰ L. M. Zhang,⁴⁰ Z. P. Zhang,⁴⁰ V. Zhilich,² T. Ziegler,³⁷ D. Žontar,^{21,15} and D. Zürcher²⁰

(The Belle Collaboration)

¹Aomori University, Aomori ²Budker Institute of Nuclear Physics, Novosibirsk ³Chiba University, Chiba ⁴Chonnam National University, Kwangju ⁵Chuo University, Tokyo ⁶University of Cincinnati, Cincinnati, Ohio 45221 ⁷University of Frankfurt, Frankfurt ⁸Gyeongsang National University, Chinju ⁹University of Hawaii, Honolulu, Hawaii 96822 ¹⁰High Energy Accelerator Research Organization (KEK), Tsukuba ¹¹Hiroshima Institute of Technology, Hiroshima ¹²Institute of High Energy Physics, Chinese Academy of Sciences, Beijing ¹³Institute of High Energy Physics, Vienna ¹⁴Institute for Theoretical and Experimental Physics, Moscow ¹⁵J. Stefan Institute. Liubliana ¹⁶Kanagawa University, Yokohama ¹⁷Korea University, Seoul ¹⁸Kyoto University, Kyoto ¹⁹Kyunqpook National University, Taequ ²⁰Swiss Federal Institute of Technology of Lausanne, EPFL, Lausanne ²¹University of Ljubljana, Ljubljana ²²University of Maribor, Maribor ²³University of Melbourne, Victoria ²⁴Nagoya University, Nagoya ²⁵Nara Women's University, Nara ²⁶National Central University, Chung-li ²⁷National Kaohsiung Normal University, Kaohsiung ²⁸National United University. Miao Li ²⁹Department of Physics, National Taiwan University, Taipei ³⁰H. Niewodniczanski Institute of Nuclear Physics, Krakow ³¹Nihon Dental College, Niigata ³²Niigata University, Niigata ³³Osaka City University, Osaka ³⁴Osaka University, Osaka ³⁵Panjab University, Chandigarh ³⁶Peking University, Beijing

³⁷Princeton University, Princeton, New Jersey 08545 ³⁸RIKEN BNL Research Center, Upton, New York 11973 ³⁹Saga University, Saga ⁴⁰University of Science and Technology of China, Hefei ⁴¹Seoul National University, Seoul ⁴²Sungkyunkwan University, Suwon ⁴³University of Sydney, Sydney NSW ⁴⁴ Tata Institute of Fundamental Research, Bombay ⁴⁵Toho University, Funabashi ⁴⁶Tohoku Gakuin University, Tagajo ⁴⁷Tohoku University, Sendai ⁴⁸Department of Physics, University of Tokyo, Tokyo ⁴⁹Tokyo Institute of Technology, Tokyo ⁵⁰Tokyo Metropolitan University, Tokyo ⁵¹ Tokyo University of Agriculture and Technology, Tokyo 52 Toyama National College of Maritime Technology, Toyama ⁵³University of Tsukuba, Tsukuba ⁵⁴ Utkal University, Bhubaneswer ⁵⁵Virginia Polytechnic Institute and State University, Blacksburg, Virginia 24061 ⁵⁶Yonsei University, Seoul

Abstract

We report the observation of a near-threshold enhancement in the $\omega J/\psi$ invariant mass distribution for exclusive $B \to K\omega J/\psi$ decays. The statistical significance of the $\omega J/\psi$ mass enhancement is estimated to be greater than 8σ . The results are obtained from a 253 fb⁻¹ data sample that contains 274 million $B\bar{B}$ pairs that were collected near the $\Upsilon(4S)$ resonance with the Belle detector at the KEKB asymmetric energy e^+e^- collider.

PACS numbers:

INTRODUCTION

B meson decays are a prolific source of charmonium particles and the large B meson samples produced at B-factories provide excellent opportunities to search for the missing charmonium states. From studies of $K_SK^-\pi^+$ systems produced in exclusive $B \to KK_SK^-\pi^+$ decays with a 44.8M $B\bar{B}$ event sample, the Belle group made the first observation of the $\eta_c(2S)$ [1]. Subsequently, with 152M $B\bar{B}$ events, the X(3872) was discovered in exclusive $B \to K\pi^+\pi^-J/\psi$ decays [2].

In this note we report on a study of $B \to K\omega J/\psi$ decays. We observe a large enhancement in the $\omega J/\psi$ mass distribution near the $\omega J/\psi$ mass threshold. These results are based on a 253 fb⁻¹ data sample that contains 274million $B\bar{B}$ pairs, collected with the Belle detector.

The Belle experiment observes B mesons produced by the KEKB asymmetric energy e^+e^- collider [3]. KEKB operates at the $\Upsilon(4S)$ resonance ($\sqrt{s} = 10.58$ GeV) with a peak luminosity of 1.39×10^{34} cm⁻²s⁻¹. The Belle detector is described in ref. [4].

EVENT SELECTION

We select events of the type $B \to K\pi^+\pi^-\pi^0 J/\psi$, with the same kaon, charged pion and J/ψ requirements as used in ref. [2]. We identify a π^0 as a $\gamma\gamma$ pair that fits the $\pi^0 \to \gamma\gamma$ hypothesis with $\chi^2 < 6$. We further require the energy asymmetry $|(E_{\gamma_1} - E_{\gamma_2})|/|(E_{\gamma_1} + E_{\gamma_2})| < 0.9$ and the π^0 center-of-mass system (cms) momentum to be greater than 180 MeV.

At the $\Upsilon(4S)$, BB meson pairs are produced with no accompanying particles. As a result, the B mesons have a total center-of-mass system (cms) energy that is equal to E_{beam} , the cms beam energy. We identify B mesons using the beam-constrained mass $M_{bc} = \sqrt{E_{beam}^2 - p_B^2}$ and the energy difference $\Delta E = E_{beam} - E_B$, where p_B is the vector sum of the cms momenta of the B meson decay products and E_B is their cms energy sum. The experimental resolution of M_{bc} is approximately 3 MeV; that for ΔE is 13 MeV for the final state used in this analysis.

We select events with $M_{bc} > 5.20$ GeV and $|\Delta E| < 0.2$ GeV. For events with multiple π^0 entries in this region, we select the $\gamma\gamma$ combination with the best χ^2 value for the $\pi^0 \to \gamma\gamma$ hypothesis. Multiple entries caused by multiple charged particle assignments are small ($\sim 4\%$) and are tolerated. The signal region is defined as 5.2725 GeV $< M_{bc} < 5.2875$ GeV and $|\Delta E| < 0.030$ GeV, which is $\simeq \pm 3\sigma$ from the central values.

Figure 1 shows a scatterplot of $M(\pi^+\pi^-\pi^0 J/\psi)$ (vertical) [5] $vs\ M(\pi^+\pi^-\pi^0)$ for selected events in the ΔE - $M_{\rm bc}$ signal region. Here a distinct vertical band corresponding to $\omega \to \pi^+\pi^-\pi^0$ is evident near $M(\pi^+\pi^-\pi^0) = 0.782$ GeV. We identify three-pion combinations with 0.760 GeV $< M(\pi^+\pi^-\pi^0) < 0.805$ GeV as candidate ω mesons.

Figure 2 shows a Dalitz plot of $M^2(\omega J/\psi)$ (vertical) vs $M^2(\omega K)$ (horizontal) for $B \to K\omega J/\psi$ candidates. There is a clustering of events near the left side of the plot, corresponding to $B \to K_X J/\psi$; $K_X \to K\omega$ events, where K_X denotes strange meson resonances such as $K_1(1270)$, $K_1(1400)$, and $K_2^*(1430)$ that are known to decay to $K\omega$. There is also a clustering of events with low $\omega J/\psi$ invariant masses near the bottom of the Dalitz plot. This clustering is the subject of the analysis reported here. We suppress $K_X \to K\omega$ events by restricting further analysis to events in the region $M(K\omega) > 1.6$ GeV, as indicated by the dotted line in Fig. 2.

Figure 3(a) shows the $M_{\rm bc}$ distribution for selected events that are in the ΔE and ω signal regions. Here the $M(\omega K) > 1.6$ GeV requirement has been applied. The curve in

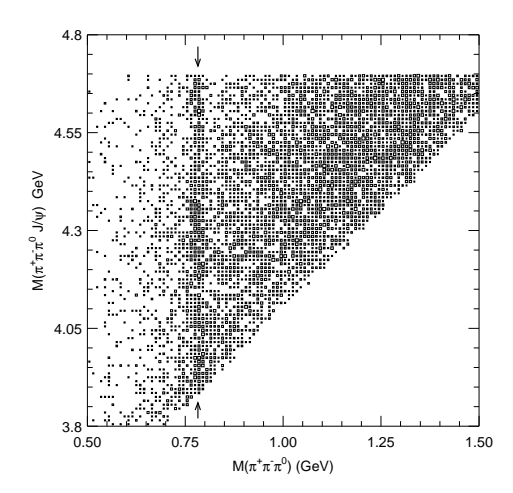


FIG. 1: Scatterplot of $M(\pi^+\pi^-\pi^0 J/\psi)$ (vertical) $vs~M(\pi^+\pi^-\pi^0)$ for events in the ΔE - $M_{\rm bc}$ signal region. The vertical band indicated by the arrows corresponds to $\omega \to \pi^+\pi^-\pi^0$ decays.

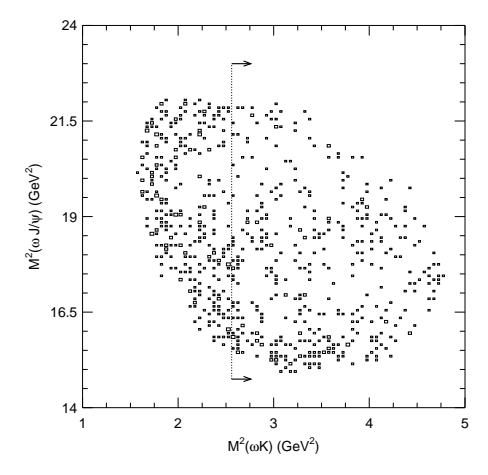


FIG. 2: The Dalitz-plot distribution for $B \to K\omega J/\psi$ candidate events.

the figure is the result of a binned likelihood fit that uses a single Gaussian for the signal and an ARGUS function [6] for the background. The fit gives a signal yield of 219 ± 24 events. Figure 3(b) shows the ΔE distribution for events in the $M_{\rm bc}$ and ω signal regions. Here the curve is the result of a fit that represents the signal with a single Gaussian and the background with a third-order polynomial. The signal yield is 196 ± 22 events. Figure 3(c) shows the $M(\pi^+\pi^-\pi^0)$ distribution for all events in the $M_{\rm bc}$ - ΔE signal region. The peak is well fitted with a Breit-Wigner with the mass and width of the $\omega(780)$, broadened by an experimental resolution of 8 MeV. Here the signal yield is 204 ± 23 events. There is reasonable consistency in the signal yield from all three distributions. In each of the figures, the signal regions are indicated by arrows.

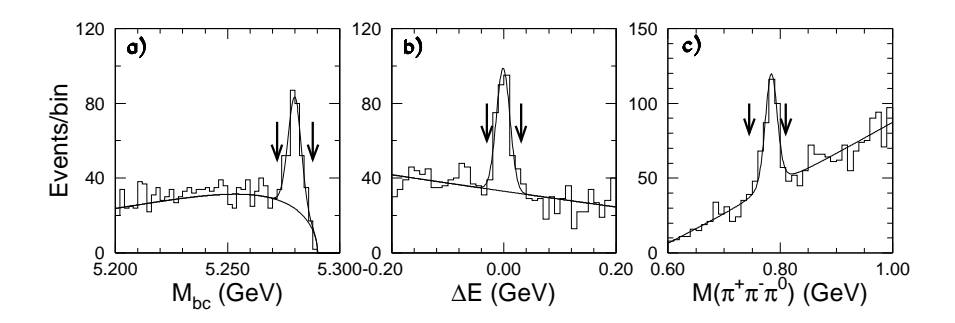


FIG. 3: (a) $M_{\rm bc}$ distributions for $B \to K\omega J/\psi$ candidates in the ΔE and $\omega \to \pi^+\pi^-\pi^0$ signal regions. (b) ΔE distribution for events in the $M_{\rm bc}$ and ω signal regions. (c) $M(\pi^+\pi^-\pi^0)$ distribution for events in the $M_{\rm bc}$ and ΔE signal regions. The curves are the results of fits described in the text; the arrows indicate the signal region for each quantity.

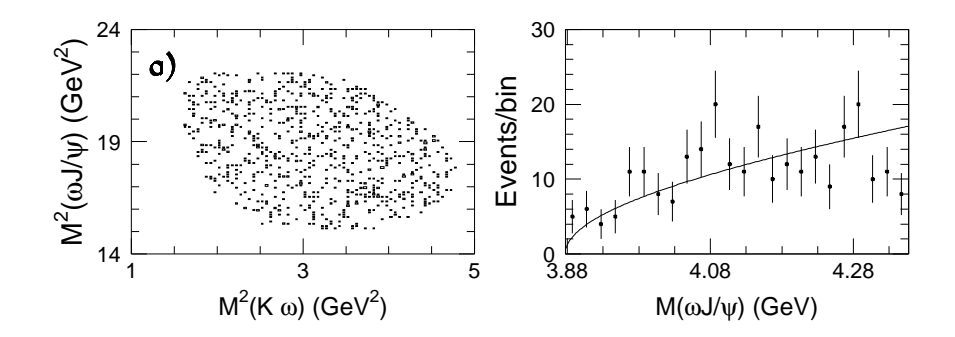


FIG. 4: **a)** The Dalitz plot distribution for phase-space MC $B \to K\omega J/\psi$ events that satisfy our selection criteria. **b)** The $M(\omega J/\psi)$ projection of selected phase-space MC events with $M(K\omega) > 1.6$ GeV. The curve is the results of a fit described in the text.

ACCEPTANCE

We generated 20 thousand $B \to K\omega J/\psi$ MC events with the three final-state particles uniformly distributed over phase-space. The Dalitz plot distribution for events that satisfy all of the selection criteria is shown in Fig. 4(a). The selected event Dalitz-plot distribution is reasonably uniform, indicating that the acceptance does not depend strongly on the final-state configuration.

Figure 4(b) shows the near-threshold $M(\omega J/\psi)$ mass projection for phase-space MC events with $M(K\omega) > 1.6$ GeV. The distribution is well fitted $(\chi^2/d.o.f. = 37.5/23)$ by a simple, monotonically increasing threshold function of the form $f(M) = A_0 q^*(M)$, where $q^*(M)$ is the momentum of the daughter particles in the $\omega J/\psi$ restframe.

THE $\omega J/\psi$ INVARIANT MASS DISTRIBUTION

The fits to the $M_{\rm bc}$ and ΔE distributions of Figs. 3(a) and (b) indicate that about half of the entries in the $M(\omega K) > 1.6$ GeV Dalitz plot region are background. To determine

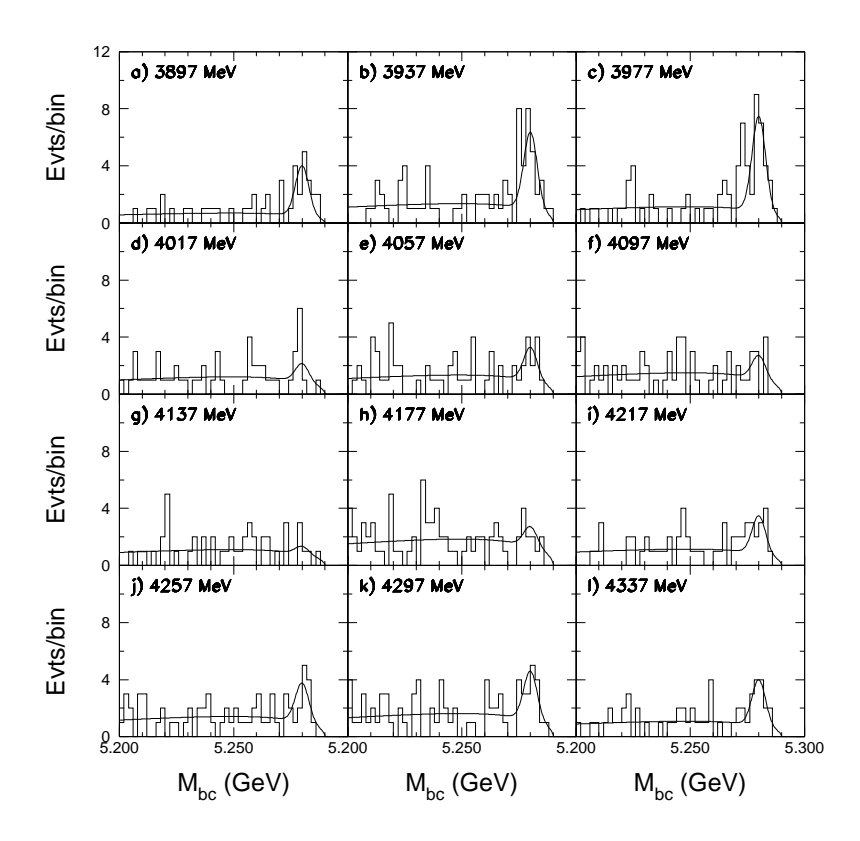


FIG. 5: $M_{\rm bc}$ distributions for 40 MeV-wide bins in $M(\omega J/\psi)$. The curves are results of fits described in the text.

the level of $B \to K\omega J/\psi$ signal events, we bin the data into 40 MeV-wide bins of $M(\omega J/\psi)$ and look for B meson signals. The histograms in Figs. 5(a)-(l) show the $M_{\rm bc}$ distributions for the twelve lowest $M(\omega J/\psi)$ mass bins.

The data show significant $B \to K\omega J/\psi$ signals in the low-mass region, especially for the mass regions covered by Figs. 5(b) and (c). We establish the $B \to K\omega J/\psi$ signal level for each $M(\omega J/\psi)$ mass bin by performing binned fits to the $M_{\rm bc}$ and ΔE distributions simultaneously for each $M(\omega J/\psi)$ region using the same signal and background functions that are used to fit the integrated distributions of Figs. 3(a) and (b). For these bin-by-bin fits, the peak positions, resolution values and background shapes are all fixed at the values that are determined from the fits to the integrated distributions. The areas of the M_{bc} and ΔE signal functions are constrained to be equal. The curves in Fig. 5 indicate the results of the fits.

RESULTS

The results of the fits to the individual bins are plotted vs $M(\omega J/\psi)$ in Figs. 6(a) and (b). An enhancement is evident around $M(\omega J/\psi) = 3940$ MeV. The curve in Fig. 6(a) is the result of a fit with the same threshold function used to fit the phase-space MC distribution of Fig. 4(b). Here the fit quality is poor $(\chi^2/dof = 133/11)$, indicating a significant deviation from phase-space; the integral of $f(\Delta M)$ over the first three bins is 16.1 events, where the

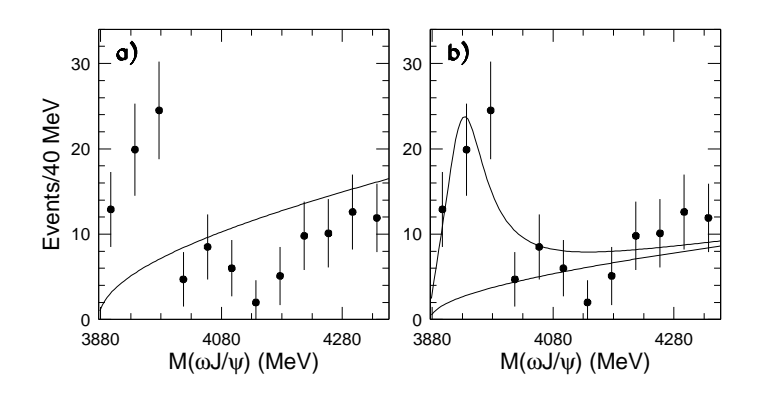


FIG. 6: $B \to K\omega J/\psi$ signal yields $vs\ M(\omega J/\psi)$. The curve in (a) indicates the result of a fit that includes only a phase-space-like threshold function. The curve in (b) shows the result of a fit that includes an S-wave Breit-Wigner resonance term.

data total is 57.3 events.

In Fig. 6(b) we show the results of a fit where we include an S-wave Breit Wigner function [7] to represent the enhancement. The fit, which has $\chi^2/dof=18.8/8$ (CL = 1.6%), yields a Breit-Wigner signal yield of 61 ± 11 events with a mass $M=3941\pm11$ MeV and a width $\Gamma=92\pm24$ MeV (statistical errors only). The BW parameters are sensitive to the shape used to model the background. If we change the background function to a second-order polynomial function in q^* that is constrained to zero at $q^*=0$, the yield increases to 81 ± 10 events, the mass changes to 3949 ± 9 MeV, the width changes to $\Gamma=112\pm25$ MeV and the fit quality improves: $\chi^2/d.o.f.=11.8/6$ (CL=6.7%).

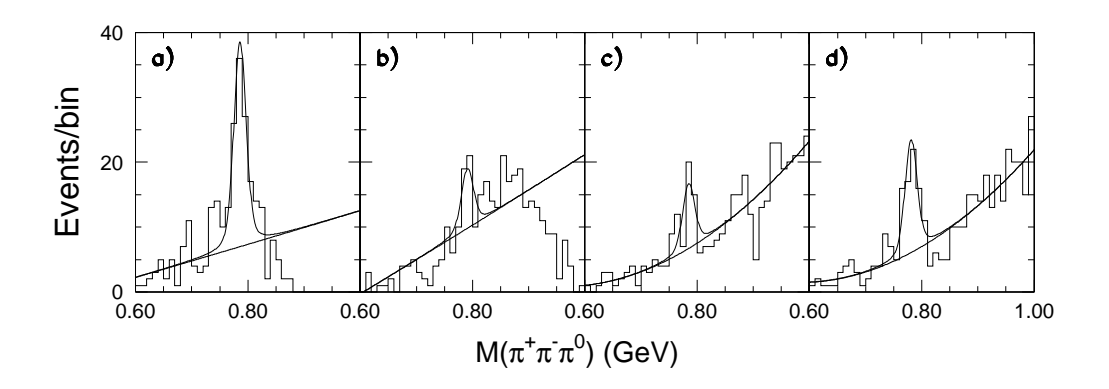


FIG. 7: $M(\pi^+\pi^-\pi^0)$ distributions for events in the M_{bc} - ΔE signal region for the $M(\omega J/\psi)$ mass regions: (a) 3877 - 3997 MeV; (b) 3997 - 4117 MeV; (c) 4117 - 4237 MeV; and (d) 4237 - 4357 MeV.

Figure 7 shows the $M(\pi^+\pi^-\pi^0)$ distributions for four $M(\omega J/\psi)$ mass bins covering 120 MeV intervals centered at (a) 3937 MeV, (b) 4057 MeV, (c) 4177 MeV and (d) 4297 MeV. The curves are results of fits to the $\omega \to \pi^+\pi^-\pi^0$ peak using functions and parameters described above. There are $\omega \to \pi^+\pi^-\pi^0$ signals in each region that track the M_{bc} - ΔE signal yields. (The absence of background on the high mass side of the ω peak in Fig. 7(a) reflects the presence of a kinematic boundary.)

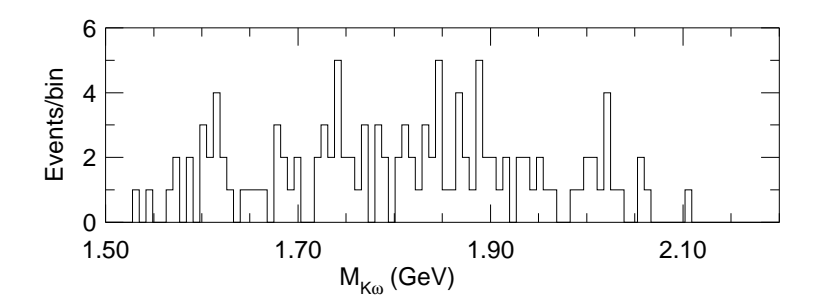


FIG. 8: The $K\omega$ invariant mass distribution for events in the M_{bc} - ΔE signal region and the $M(\omega J/\psi)$ mass enhancement (3877 MeV < $M(\omega J/\psi)$ <3997 MeV).

Figure 8 shows the $K\omega$ invariant mass distribution for $M_{\rm bc}$ - ΔE signal region events in the region of the $M(\omega J/\psi)$ enhancement (3877 MeV< $M(\omega J/\psi)$ <3997 MeV). The events appear to be distributed uniformly across the available phase space and there is no evidence for any $K\omega$ mass structure that might be producing the observed $\omega J/\psi$ mass enhancement by some kind of kinematic reflection.

Product branching fraction

To determine a branching fraction, we use the BW fit shown in Fig. 6(b) to establish the event yield of the observed enhancement. Monte Carlo simulations of a narrow state with mass 3940 MeV decaying into $\omega J/\psi$ are used to estimate detection efficiencies of 3.5% and 1.9% for $B \to K^+ \omega J/\psi$ and $K^0 \omega J/\psi$, respectively. We assume the same branching fraction for charged and neutral B mesons. We use PDG [8] values for the $K_S \to \pi^+ \pi^-$, $\omega \to \pi^+ \pi^- \pi^0$ and $J/\psi \to \ell^+ \ell^-$ branching fractions. For the data set used for this analysis, the number of $B\bar{B}$ pairs is 274 million. We find a product branching fraction (here we denote the enhancement as "Y")

$$\mathcal{B}(B \to K \text{"}Y\text{"})\mathcal{B}(\text{"}Y\text{"} \to \omega J/\psi) = (5.0 \pm 0.9 \pm 1.6) \times 10^{-5},$$
 (1)

where the second error is systematic and includes the uncertainties in the choice of the shape of the background under the enhancement.

Significance

We estimate the significance of the enhancement in two ways. The fitted phase-space-like background function shown in Fig. 6(a) has an integrated area under the lowest three data points of 16.1 ± 1.4 events; the total number of observed events in the same three bins is 57.3. This corresponds to a signal significance of more than 9σ . The fit in Fig. 6(a) has $-2 \ln \mathcal{L} = 93.1$; the fit with a BW "signal" in Fig. 6(b) improves this to $-2 \ln \mathcal{L} = 20.7$. This translates into a significance of more than 8σ .

DISCUSSION

We have observed a strong near-threshold enhancement in the $\omega J/\psi$ mass spectrum in exclusive $B \to K\omega J/\psi$ decays. The enhancement peaks well above threshold and is broad [9]: if treated as a single resonance, we find a mass of 3941 \pm 11 MeV and a total width $\Gamma = 92 \pm 24$ MeV. It is expected that any "normal" $c\bar{c}$ charmonium meson with this mass would dominantly decay to $D\bar{D}$ and/or $D\bar{D}^*$; hadronic charmonium transitions should have minuscule branching fractions. The properties of the observed enhancement are similar to those of $c\bar{c}$ -gluon charmonium hybrid states that occur in Lattice QCD [10] and are expected to be produced in B-meson decays [11]. However, the Lattice calculations indicate that the lightest hybrid states have masses around 4400 MeV, well above the mass of the enhancement reported here.

Acknowledgments

We thank the KEKB group for the excellent operation of the accelerator, the KEK Cryogenics group for the efficient operation of the solenoid, and the KEK computer group and the National Institute of Informatics for valuable computing and Super-SINET network support. We acknowledge support from the Ministry of Education, Culture, Sports, Science, and Technology of Japan and the Japan Society for the Promotion of Science; the Australian Research Council and the Australian Department of Education, Science and Training; the National Science Foundation of China under contract No. 10175071; the Department of Science and Technology of India; the BK21 program of the Ministry of Education of Korea and the CHEP SRC program of the Korea Science and Engineering Foundation; the Polish State Committee for Scientific Research under contract No. 2P03B 01324; the Ministry of Science and Technology of the Russian Federation; the Ministry of Education, Science and Sport of the Republic of Slovenia; the National Science Council and the Ministry of Education of Taiwan; and the U.S. Department of Energy.

- * on leave from Nova Gorica Polytechnic, Nova Gorica
- [1] S.K. Choi et al. (Belle Collaboration), Phys. Rev. Lett. 89, 102001 (2002).
- [2] S.K. Choi et al. (Belle Collaboration), Phys. Rev. Lett. 91, 262001 (2003).
- [3] S. Kurokawa and E. Kikutani, Nucl. Instr. and. Meth. A 499, 1 (2003).
- [4] A. Abashian *et al.* (Belle Collaboration), Nucl. Instr. and Meth. A **479**, 117 (2002) and Y. Ushiroda (Belle SVD2 Group), Nucl. Instr. and Meth. A **511**, 6 (2003).
- [5] We require $|M(\ell^+\ell^-) M_{J/\psi}| < 0.02$ GeV and reduce lepton momentum resolution effects by defining $M(\pi^+\pi^-\pi^0J/\psi) \equiv M(\pi^+\pi^-\pi^0\ell^+\ell^-) M(\ell^+\ell^-) + M_{J/\psi}$.
- [6] H. Albrecht et al. (ARGUS Collaboration), Phys. Lett. B 299, 304 (1989).
- [7] We use the form $\frac{\Gamma(q^*/q_0)}{(M^2-M_0^2)^2+(M_0\Gamma(q^*/q_0))^2}$, where M_0 is the peak mass and $q_0=q^*(M=M_0)$.
- [8] S. Eidelman et al., Phys. Lett. B 592, 1 (2004).
- [9] The $M(\omega J/\psi)$ mass resolution is $\simeq 6$ MeV, much narrower than the observed enhancement.
- [10] See, for example, S. Godfrey and J. Napolitano, Rev. Mod. Phys. **71**, 1411 (1999), and references cited therein.
- [11] F.E. Close and S. Godfrey, Phys. Lett. B **574**, 210 (2003).